

Nonlocal Stabilization of Nonlinear Beams in a Self-Focusing Atomic Vapor

S. Skupin,¹ M. Saffman,² and W. Królikowski¹

¹Research School of Physical Sciences and Engineering, Australian National University, Canberra, ACT 0200, Australia

²Department of Physics, University of Wisconsin, 1150 University Avenue, Madison, Wisconsin 53706, USA

(Received 20 December 2006; published 29 June 2007)

We show that ballistic transport of optically excited atoms in an atomic vapor provides a nonlocal nonlinearity which stabilizes the propagation of vortex beams and higher order modes in the presence of a self-focusing nonlinearity. Numerical experiments demonstrate stable propagation of higher order nonlinear states (dipole, vortices, and rotating azimuthons) over a hundred diffraction lengths, before dissipation leads to decay of these structures.

DOI: [10.1103/PhysRevLett.98.263902](https://doi.org/10.1103/PhysRevLett.98.263902)

PACS numbers: 42.65.Tg, 32.80.-t, 42.65.Sf

The propagation and dynamics of localized nonlinear waves is a subject of great interest in a range of physical settings stretching from nonlinear optics to plasmas and ultracold atomic gases [1,2]. The structure and stability of nonlinear optical modes is determined by the interplay between the radiation field and the material nonlinearity [3]. The nonlinear response can be described by an optically induced change in the refractive index n , which is typically approximated as a local function of the wave intensity, i.e., $n(\mathbf{r}) = n(I(\mathbf{r}))$. However, in many real physical systems the nonlinear response is spatially nonlocal which means that the refractive index depends on the beam intensity in the neighborhood of each spatial point. This can be phenomenologically expressed as $n(\mathbf{r}) = \int d\mathbf{r}' K(\mathbf{r}, \mathbf{r}') I(\mathbf{r}')$, where the response kernel K depends on the particular model of nonlocality [4].

It has been shown that nonlocality drastically affects the stationary structure and dynamics of spatial solitons, leading to such effects as collapse arrest of high intensity beams and stabilization of otherwise unstable complex solitonic structures [5–8]. Nonlocality is often the consequence of transport processes which include atom or heat diffusion in atomic vapors [9], plasma [10] and thermal media [11], or charge transport in photorefractive crystals [12]. In addition, long range interactions are responsible for a nonlocal response in liquid crystals [13] or dipolar Bose-Einstein condensates [14].

Hot atomic vapors are an important and widely used nonlinear medium. The nonlocal nonlinear response of atomic vapors has previously only been associated with state dependent transport of ground state atoms which possess a multilevel structure [9]. In this Letter we introduce a new mechanism of nonlocality which is provided by the ballistic transport of excited atoms and is important even for the simplest case of an idealized two-level atom. We show using parameters representative of beam propagation in rubidium vapor that ballistic transport plays a dramatic role leading to stabilization of otherwise unstable vortex modes and rotating solitonic structures in the presence of a self-focusing nonlinearity.

We start the theoretical development by briefly recalling the main features of beam propagation in a hot atomic vapor. We consider a scalar traveling wave $E = \frac{\mathcal{E}(x,y,z)}{2} e^{i(kz - \omega t)} + \text{c.c.}$ For all parameters of interest the refractive index is $n \simeq 1$ so the wave intensity is $I \simeq \frac{\epsilon_0 c}{2} |\mathcal{E}|^2$. In the slowly varying envelope approximation the paraxial wave equation is

$$\frac{\partial \mathcal{E}}{\partial z} - \frac{i}{2k} \nabla_{\perp}^2 \mathcal{E} = -\frac{k\chi_0''}{2} \mathcal{E} + i\frac{k}{2} [\chi_{\text{nl}}'(I) + i\chi_{\text{nl}}''(I)] \mathcal{E}, \quad (1)$$

where $k = \omega/c$. The susceptibilities χ' and χ'' depend on atomic parameters. We assume a two-level atomic model for which the scattering cross section is $\sigma = (3\lambda_a^2/2\pi) \times (1 + 4\Delta_0^2/\gamma^2 + I/I_s)^{-1}$, and the index of refraction is $n = 1 - n_a(\sigma/k)(\Delta_0/\gamma)$, where λ_a is the transition wavelength, n_a is the atomic density, γ is the full width at half maximum (FWHM) natural linewidth, $\Delta_0 = \omega - \omega_a$ is the detuning between the optical frequency ω and the atomic transition frequency $\omega_a = 2\pi c/\lambda_a$, and I_s is the saturation intensity. For a probe beam propagating along \hat{z} in a hot vapor we make the replacement $\Delta_0 \rightarrow \Delta = \Delta_0 - kv_z$, where v_z is the z component of the atomic velocity. Averaging over a Maxwell-Boltzmann velocity distribution at temperature T gives the linear and nonlinear susceptibilities [15] $\chi_0'' = \chi_0 \text{Im}[Z(a + ib)]$,

$$\chi_{\text{nl}}^{\text{loc}}(I) = \chi_0 \{ \text{Re}[Z(a + ib_I)] - \text{Re}[Z(a + ib)] \}, \quad (2a)$$

$$\chi_{\text{nl}}^{\text{loc}}(I) = \chi_0 \left\{ \frac{\text{Im}[Z(a + ib_I)]}{\sqrt{1 + I/I_s}} - \text{Im}[Z(a + ib)] \right\}, \quad (2b)$$

where $\chi_0 = n_a 6\pi b c^3 / \omega_a^3$, $a = 2b\Delta_0/\gamma$, $b = \sqrt{\ln 2} \gamma / \omega_D$, $b_I = b\sqrt{1 + I/I_s}$, and $\omega_D = k\sqrt{8 \ln 2 k_B T/m}$ is the FWHM of the Doppler profile for an atom of mass m . The plasma dispersion function is given by $Z(z) = i\sqrt{\pi} e^{-z^2} \text{Erfc}(-iz)$, where $\text{Erfc}(z) = 1 - (2/\sqrt{\pi}) \int_0^z dt e^{-t^2}$ is the complementary error function.

For broad optical beams numerical solutions of Eqs. (1) and (2) give an accurate description of propagation effects in an atomic vapor. The physical effect leading to the nonlinear optical response is the transfer of population

from the ground to the excited state and the creation of coherence between these states. Although motional effects are accounted for as regards the Doppler smearing of the transition frequency, atomic motion also results in transport of excited atoms which leads to a nonlocal response. The degree of nonlocality depends on the characteristic length scales associated with the transport of excited state atoms. The first length scale is the mean free path atoms travel before a Rb-Rb collision occurs. This is given by $\ell_c = (\sqrt{2}n_a\sigma)^{-1}$, where σ is the collisional cross section. For collisions of ground state Rb atoms we use [16] $\sigma^{(g-g)} = 2.5 \times 10^{-17} \text{ m}^2$. The cross section for collisions between excited and ground state collisions is much larger since these collisions occur via a long range dipole-dipole interaction [17]. The energy averaged cross section is $\sigma^{(g-e)} \sim \frac{1.8 \times 10^{-14}}{\sqrt{T}} \text{ K}^{1/2} \text{ m}^2$. The second length scale is $\ell_d = \tilde{v}\tau$, which is the distance traveled by an atom moving at the most probable speed $\tilde{v} = \sqrt{2k_B T/m}$ in the $1/e$ lifetime τ of the excited state. For the $^{87}\text{Rb } 5P_{3/2}$ level $\tau \approx 26 \text{ ns}$. Figure 1 shows that for $T < 155^\circ \text{C}$ the ballistic transport length for excited atoms is $\ell_d \sim 7.5 \mu\text{m}$ and $\ell_d < \ell_c^{(g-e)}$, $\ell_c^{(g-g)}$. Thus, for these temperatures, transport of excited atoms is ballistic with a length scale of ℓ_d . We note that the density at $T = 155^\circ \text{C}$ is $n_a = 10^{20} \text{ m}^{-3}$, which is several orders of magnitude smaller than densities for which nonlocal effects due to the Lorentz local field are important [18].

We wish to find an expression for the nonlocal material response that depends on the parameters τ and \tilde{v} . We write the total atomic density $n_a = n_g + n_e$ as the sum of ground and excited state partial densities and introduce rate equations of the form $\frac{\partial n_{g,e}}{\partial t} = \mp [\frac{I\alpha(I)}{\hbar\omega} - \gamma n_e] + \mathcal{L}_{g,e}[n_{g,e}]$, where \mathcal{L}_g , \mathcal{L}_e are, as yet unknown, linear operators for ground and excited state atoms and $\alpha(I) = k[\chi_0'' + \chi_{\text{nl}}''(I)]$ is the absorption coefficient. If we assume that the total density is unchanged by the presence of the laser field (this is a reasonable assumption in hot vapors) we must have

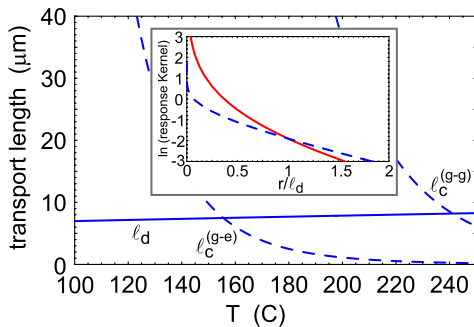


FIG. 1 (color online). Characteristic length scales $\ell_c^{(g-g)}$, $\ell_c^{(g-e)}$, and ℓ_d in a Rb vapor cell as a function of temperature. The inset shows the logarithm of the ballistic response function $\sim (\ell_d/r) \int_0^\infty d\xi e^{-r/(\tilde{v}\xi)} e^{-\xi^2}$ (solid red line) and the response function $K_0(r/\ell_d)$ for a 2D diffusive nonlocal equation [8] (dashed blue line) as a function of r/ℓ_d . The response functions have been scaled to be equal at $r = \ell_d$.

$\mathcal{L}_g[n_g] = -\mathcal{L}_e[n_e]$. If excited state transport were a diffusive process we would have $\mathcal{L}_e[n_e] = D_e \nabla^2 n_e$ and on dimensional grounds $D_e \sim (\tilde{v}\tau)^2/\tau \sim \ell_d^2/\tau$.

The situation in the ballistic regime is different. The collisionless Boltzmann equation for the density of excited atoms is $\frac{dn_e}{dt} = \frac{\partial n_e}{\partial t} + \mathbf{v} \cdot \nabla_{\mathbf{r}} n_e$. Working within the paraxial approximation we are interested in the two-dimensional problem where $\mathbf{r} = x\hat{x} + y\hat{y}$ and $\mathbf{v} = v_x\hat{x} + v_y\hat{y}$. The Green function is found by solving $\frac{dn_e}{dt} = \delta(t)n_0(\mathbf{r}, \mathbf{v})$ with $n_0(\mathbf{r}, \mathbf{v}) = \delta(\mathbf{r}_0)f(\mathbf{v})$, and $f(\mathbf{v}) = (m/2\pi k_B T)e^{-v^2/\tilde{v}^2}$, the two-dimensional thermal velocity distribution. Integrating the resulting Green function over the velocity distribution and accounting for the fact that the excitation decays with rate γ gives the spatiotemporal Green function $G_r(\mathbf{r}, t; \mathbf{r}_0, t_0; \gamma) = \frac{1}{\pi\gamma^2\ell_d^2} \times \frac{e^{-\gamma(t-t_0)}}{(t-t_0)^2} e^{-|\mathbf{r}-\mathbf{r}_0|^2/(\tilde{v}^2(t-t_0)^2)}$. The Green function for the steady state response is

$$G(\mathbf{r}, \mathbf{r}_0; \gamma) = \frac{1}{\pi\tilde{v}r} \int_0^\infty d\xi e^{-\gamma r/(\tilde{v}\xi)} e^{-\xi^2}, \quad (3)$$

where $r = |\mathbf{r} - \mathbf{r}_0|$ and the density of excited atoms due to the intensity $I = I_0\delta(\mathbf{r}_0)$ is $n_e(\mathbf{r}) = G(\mathbf{r}, \mathbf{r}_0; \gamma) \frac{\alpha(I_0)I_0}{\hbar\omega}$.

The result is plotted in the inset of Fig. 1 as a function of the scaled coordinate r/ℓ_d . We see, not unexpectedly, that the ballistic response falls off much more rapidly than the diffusive response. Note that $\int dr G(\mathbf{r}, 0, \gamma) = 1/\gamma$, since the time integrated response exponentially weights the input over a time window $\tau = 1/\gamma$. The spatial Fourier transform of the Green function is given by $\mathcal{F}[G] = \frac{\sqrt{\pi}}{\gamma} \times \frac{e^{1/(k\ell_d)^2} \text{Erfc}[1/(k\ell_d)]}{k\ell_d}$, which is well behaved with $\lim_{k \rightarrow 0} \mathcal{F}[G] = 1/\gamma$.

To complete the theoretical formulation of the wave propagation problem we need to calculate the nonlocal structure of the susceptibility χ_{nl} . When I is spatially varying we can use the Green function to write the stationary response as

$$\chi_{\text{nl}}^{\text{nonloc}}(\mathbf{r}) = \gamma \int d\mathbf{r}_0 G(\mathbf{r}, \mathbf{r}_0; \gamma) \chi_{\text{nl}}^{\text{loc}}[I(\mathbf{r}_0)]. \quad (4)$$

The real part of the susceptibility is proportional to the coherence between ground and excited states which decays with rate $\gamma/2$ so

$$\chi_{\text{nl}}^{\text{nonloc}}(\mathbf{r}) = \frac{\gamma}{2} \int d\mathbf{r}_0 G(\mathbf{r}, \mathbf{r}_0; \gamma/2) \chi_{\text{nl}}^{\text{loc}}[I(\mathbf{r}_0)]. \quad (5)$$

Equations (4) and (5) and the wave Eq. (1) constitute a full description of time-independent wave propagation in a two-level atomic vapor including Doppler broadening and transport induced nonlocality.

The question of whether or not the ballistic transport is sufficient to stabilize nonlinear modes can be investigated numerically. A typical approach would involve linear stability analysis which considers the original propagation equations linearized around the stationary solutions. However, such a technique does not provide any information on

structural stability, especially when linear and nonlinear losses are not negligible. Therefore, in this work we employed direct beam propagation simulations to determine stability properties of stationary solutions of Eqs. (1), (4), and (5). Stable soliton propagation in numerical experiments where the initial beam is perturbed by noise does not constitute a rigorous proof of stability but does provide strong support for the existence of observable nonlinear modes in laboratory experiments. We use parameters corresponding to off-resonant propagation in a high temperature Rb cell ($\lambda = 780$ nm, $\gamma/2\pi = 6.07$ MHz, $\Delta_0/2\pi = 1.46$ GHz, $I_s = 16.7$ W/m², $T \approx 155$ °C, $n_a = 10^{20}$ m⁻³, $\ell_d = 7.5$ μ m), which result in the dimensionless parameters $a = 4$, $b = 0.0083$, and $\chi_0 = 0.03$. We used this set throughout all the simulations presented in this Letter.

In the conservative system ($\chi''_0 = \chi''_{nl} = 0$) all simulated soliton modes which included the fundamental soliton state, single charged vortex, dipole soliton, and double-charged vortex turned out to be stable if the power $P = \int I(\mathbf{r})d\mathbf{r}$, is high enough. At least for the latter two modes this is quite remarkable, since they are known to be unstable (or only stable in a small power window) for other nonlocal models [8,19,20]. We attribute this enhanced stabilization to the combination of nonlocality and nonlinear saturation. In fact, we inserted an artificial nonlinear saturation in the nonlocal thermal model used in Ref. [19] and found the same effect. In contrast, nonlinear saturation without nonlocality does not stabilize higher order nonlinear modes [21]. The local Eqs. (1) and (2) feature a stable ground state only.

Figure 2 illustrates both saturation and nonlocality for the nonlocal single charged vortex mode. If we consider only the saturation effect shown in Fig. 2(a), the resulting nonlinear index is the dashed blue line in Fig. 2(b). Together with the nonlocal kernel G [red line in the inset of Fig. 1] we get the solid blue line, showing some filling in of the central dip in the index profile, and the formation of a broader “nonlocal waveguide.”

The limiting mechanism with respect to long distance propagation of higher order nonlocal nonlinear modes is not destabilization but dissipation. The action of both χ''_0

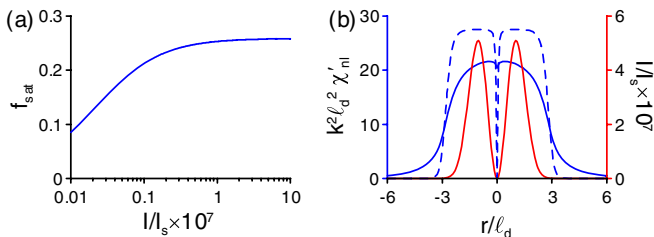


FIG. 2 (color online). (a) Saturation function $f_{\text{sat}} = \text{Re}[Z(a + ib)] - \text{Re}[Z(a + ib)]$ for $a = 4$ and $b = 0.0083$. (b) Nonlocal single charged vortex mode with power $P \approx 0.4$ W (red line and red axis). The solid blue line shows the *nonlocal* nonlinear index χ'_{nl} computed from Eq. (5), the dashed blue line the *local* one computed from Eq. (2a) (blue axis).

and χ''_{nl} is not negligible over one diffraction length $z_d = 2k\ell_d^2$ [22]. As an illustrative example, the propagation of the *nonlocal* single charged vortex mode, is shown in Fig. 3(a). As input power we use about 0.4 W. Note the clearly visible influence of the nonlinear term χ_{nl} in the blue power curve. The nonlocal vortex survives a propagation distance of more than $150z_d$ [see Fig. 3(b)]. For comparison, the propagation of the *local* vortex with the same input power is shown in dashed lines in Fig. 3(a). This vortex disintegrates after less than $15z_d$ [see Fig. 3(d)]. Hence, we clearly see that the stabilization is due to nonlocality. With the same input power of about 0.4 W, we also observed a robust nonlocal dipole [see Fig. 3(e)] and double-charged vortex [see Fig. 3(f)].

The key feature enabling robust nonlocal dissipative propagation over a hundred diffraction lengths is the above mentioned stability for high powers. Starting in the stable

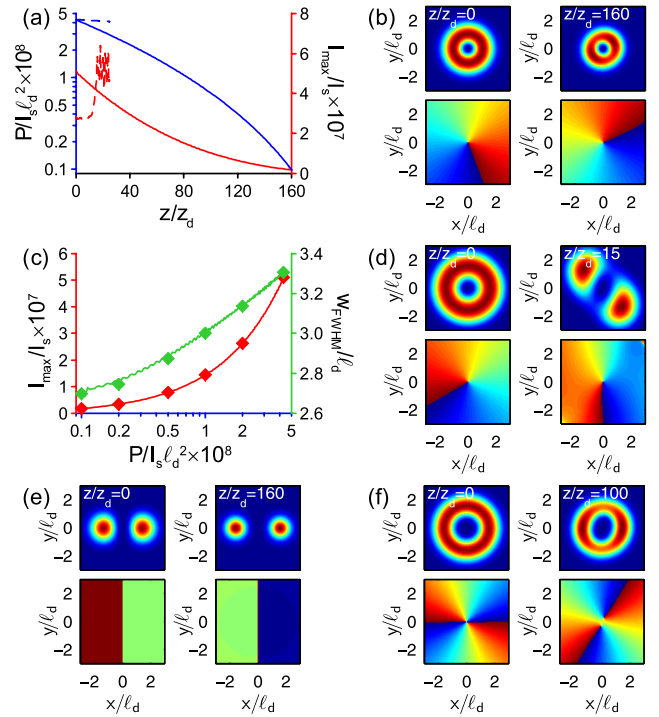


FIG. 3 (color online). (a) Nonlocal (solid lines) and local (dashed lines) dissipative propagation of the single charged vortex mode with input power 0.4 W. The blue lines and blue axis show the beam power, the red lines and red axis the maximal intensity versus propagation distance. (b) Intensity and phase distribution of the nonlocal single charged vortex at input $z = 0$ and at $z = 160z_d$ just before it decays. (c) Maximal intensity (red) and FWHM (green) of the nonlocal single charged vortex as a function of beam power. The solid lines are computed upon propagation, the diamonds from stationary numerical solutions of the conservative problem. (d) Intensity and phase distribution of the local single charged vortex at $z = 0$ and at $z = 15z_d$ when it decays. (e) Intensity and phase distribution of the nonlocal dipole mode at $z = 0$ and at $z = 160z_d$ just before it decays. (f) Same for the nonlocal double-charged vortex at $z = 0$ and at $z = 100z_d$.

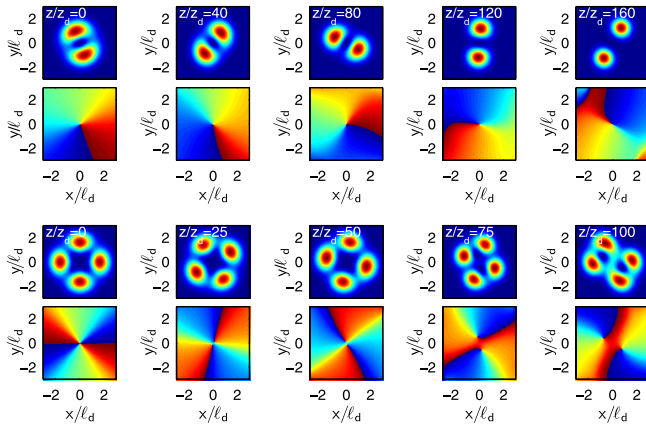


FIG. 4 (color online). Dissipative propagation of a dipole azimuthon (upper row) and quadrupole azimuthon (lower row). In both cases the input power was about 0.4 W and the modulation depth $\kappa \approx 0.5$.

power regime, dissipation makes the nonlinear mode “glide down” the family branch until it reaches powers in the unstable regime. Figure 3(c) confirms this property by comparing maximal intensity and FWHM obtained upon propagation with values found from exact numerical solution of the conservative problem using the method described in [8].

To complete our analysis of experimentally relevant nonlinear states we now consider a more general class of solutions, the so called azimuthons [23]. These are spatially rotating structures (rotation frequency Ω) described by the ansatz $\mathcal{E}(r, \phi, z) = U(r, \phi - \Omega z) \exp(i\beta z)$ in the conservative system. For $\Omega = 0$, azimuthons become ordinary (nonrotating) solitons with propagation constant β . The simplest family of azimuthons represents the transition from a dipole soliton to a single charged vortex soliton (for fixed propagation constant β). The single charged vortex is composed of two equal amplitude dipole-shaped components with relative phase of $\pi/2$. If these two components have different amplitudes they constitute an azimuthon (or rotating dipole). As pointed out in [23], the rotation frequency Ω is determined by the amplitude ratio of the two constituent modes (modulation depth $\kappa = |\max \text{Re} U - \max \text{Im} U| / \max |U|$) and, of course, the propagation constant β .

In Fig. 4 we show a few snapshots of the dissipative propagation of two azimuthons, namely, rotating dipole and quadrupole modes. As input condition we used the single- and double-charged vortices with appropriate amplitude modulation. In spite of the very rough input shapes, both rotating states survive propagation over distances comparable with those of the vortices. It is worth noticing that as power and modulation depth κ of these azimuthons decrease due to dissipation, their angular frequency continuously varies upon propagation.

In conclusion, we have shown that ballistic transport of optically excited atoms in a thermal vapor provides a generic nonlocal nonlinearity which can stabilize the

propagation of vortices and other higher order modes in a self-focusing medium. For sufficiently high power we found a stable dipole mode, single and double-charged vortices, and related rotating azimuthons. In realistic models dissipation is not negligible. Nevertheless, numerical experiments using experimentally accessible parameters demonstrate robust propagation over a hundred or more diffraction lengths. This is possible due to adiabatic conversion into solitons with lower power.

Simulations were performed on the SGI Altix cluster of the Australian Partnership for Advanced Computing.

- [1] N.N. Akhmediev and A. Ankiewicz, *Solitons-Nonlinear Pulses and Beams* (Chapman and Hall, London, 1997).
- [2] J. Denschlag *et al.*, *Science* **287**, 97 (2000); K. E. Strecker *et al.*, *Nature (London)* **417**, 150 (2002).
- [3] Yu. S. Kivshar and G. Agrawal, *Optical Solitons: From Fibers to Photonic Crystals* (Academic, San Diego, 2003).
- [4] A. Snyder and J. Mitchell, *Science* **276**, 1538 (1997).
- [5] I. A. Kolchugina, V. A. Mironov, and A. M. Sergeev, *JETP Lett.* **31**, 304 (1980); V. A. Mironov, A. M. Sergeev, and E. M. Sher, *Sov. Phys. Dokl.* **26**, 861 (1981).
- [6] W. Królkowski *et al.*, *Phys. Rev. Lett.* **80**, 3240 (1998).
- [7] W. Królkowski *et al.*, *J. Opt. B* **6**, S288 (2004); D. Briedis *et al.*, *Opt. Express* **13**, 435 (2005); A. Dreischuh *et al.*, *Phys. Rev. Lett.* **96**, 043901 (2006).
- [8] S. Skupin *et al.*, *Phys. Rev. E* **73**, 066603 (2006).
- [9] A. C. Tam and W. Happer, *Phys. Rev. Lett.* **38**, 278 (1977); D. Suter and T. Blasberg, *Phys. Rev. A* **48**, 4583 (1993).
- [10] A. G. Litvak *et al.*, *Sov. J. Plasma Phys.* **1**, 31 (1975).
- [11] F. W. Dabby and J. R. Whinnery, *Appl. Phys. Lett.* **13**, 284 (1968); S. A. Akhmanov *et al.*, *IEEE J. Quantum Electron.* **4**, 568 (1968).
- [12] A. A. Zozulya and D. Z. Anderson, *Phys. Rev. A* **51**, 1520 (1995).
- [13] C. Conti, M. Peccianti, and G. Assanto, *Phys. Rev. Lett.* **91**, 073901 (2003).
- [14] L. Santos *et al.*, *Phys. Rev. Lett.* **85**, 1791 (2000); P. Pedri and L. Santos, *Phys. Rev. Lett.* **95**, 200404 (2005).
- [15] D. H. Close, *Phys. Rev.* **153**, 360 (1967).
- [16] S. Bali *et al.*, *Phys. Rev. A* **60**, R29 (1999).
- [17] E. L. Lewis, *Phys. Rep.* **58**, 1 (1980).
- [18] J. J. Maki *et al.*, *Phys. Rev. Lett.* **67**, 972 (1991).
- [19] A. I. Yakimenko, Y. A. Zaliznyak, and Y. Kivshar, *Phys. Rev. E* **71**, 065603 (2005).
- [20] V. M. Lashkin, A. I. Yakimenko, and O. O. Prikhodko, arXiv:nlin.PS/0607062v3; A. I. Yakimenko, V. M. Lashkin, and O. O. Prikhodko, *Phys. Rev. E* **73**, 066605 (2006).
- [21] In the regime of strong saturation, the azimuthal instability is slowed down by effective decrease of the nonlinear response. See, for instance, M. S. Bigelow, P. Zerom, and R. W. Boyd, *Phys. Rev. Lett.* **92**, 083902 (2004).
- [22] Since typical transverse length scales of the nonlinear modes under consideration are of the order ℓ_d , this definition of the diffraction length makes sense.
- [23] A. S. Desyatnikov, A. A. Sukhorukov, and Y. S. Kivshar, *Phys. Rev. Lett.* **95**, 203904 (2005).